Optimization of triangular lattice defect in dynamic photonic crystal structures for optical storage and processing

Mostafa Shalaby[a], A. K. AboulSeoud[a,b], Moustafa H. Aly[a], Amr Marzouk[c]
[a]Arab Academy for Science, Technology and Maritime Transport, Alexandria, Egypt
[b]University of Alexandria, Alexandria, Egypt
[c]Simon Fraser University, Surrey, Canada

ABSTRACT

A triangular lattice GaAs photonic crystal structure was proposed in a previous work [1] for optical storage in a dynamic modulation process. This work presents a defect optimization of this tunable coupled resonator array. Preserving translational invariance and adiabaticity, this structure exhibits an optical analogue to electromagnetic induced transparency. This triangular lattice structure shows an advantage over the previously proposed square one [2, 3] in compressing higher bandwidth pulses. The main problem of this structure is the introduction of higher group-velocity dispersion. In the present work, the structure is redesigned so as to change the operating range of frequency for the propagating pulse. In this way, the group-velocity dispersion is eliminated to values close to that of the square lattice structure. The final design, therefore, combines both higher compressible bandwidth and lower group-velocity dispersion in addition to a fabrication advantage.

Keywords: Dynamic structures, temporal coupled mode theory, optical storage, group-velocity dispersion, triangular lattice, refractive index modulation.

1. INTRODUCTION

Development of dynamic structures for optical storage represents one of the recent advances in the area of photonic crystals. These structures make good use of the fascinating properties of photonic crystals in controlling light. A tunable coupled resonator array structure was proposed for dynamic tuning of the bandwidth of optical pulses [3]. In this structure, the bandwidth is adjusted to be large enough to accommodate the optical pulse. When it is completely inside the structure, the transmission properties of the structure are tuned dynamically. Under appropriate conditions, the bandwidth of the pulse can be reduced to zero. By cascading such tunable band pass filters, it is possible to reduce the velocity of a propagating pulse to zero and even to time reverse it. The pulse can then be kept in the structure indefinitely. This process can then be reversed and the pulse is released. The system therefore behaves as both a tunable band pass filter and a tunable delay element [3]. This stop-freeze-release process allows for new possibilities for optical storage and processing.

The original structure used to validate the theory is based on a two dimensional square lattice structure [3, 4]. In a previous work [1], a triangular structure was suggested instead. This triangular structure offers an advantage over the square one. It represents a better approximation to the ideal case of spherical Brillouin zone in two dimensions. This structure shows higher capabilities for bandwidth compression [1] especially when used with GaAs. However, this structure has two main disadvantages; it requires a longer waveguide length and it shows higher group-velocity dispersion. While the former can be compromised with the required system specifications [1], the latter needs more consideration. In the present work, the triangular lattice dynamic structure is revisited. The original model is redesigned so as to reduce the group-velocity dispersion while maintaining higher bandwidth compression capabilities.

Figure 1 shows two unit cells of the basic system for light manipulation. Each unit cell consists of a waveguide side coupled to two cavities [5]. The two sufficient conditions for dynamic refractive index modulation are the translational invariance and adiabaticity [5-7]. It has been shown [1] that using a triangular lattice instead of a square one will not violate any of them. The single mode waveguide is created here by removing a single row of dielectric rods. In previous works [1-3], the single mode cavity was obtained by reducing both refractive index and radius of a single rod. By modulating the refractive index of this system, the resonance frequencies of the unit cell cavities can be varied creating

Photonics North 2009, edited by Réal Vallée, Proc. of SPIE Vol. 7386, 73862D

two cavities (in each unit cell) with resonance frequencies of $\omega_{1,2}=\omega_o\pm\delta\omega/2$ [6], $\delta\omega$ is the signal bandwidth. In both square and triangular lattice structures, both cavities have the same symmetry and the system supports nonorthogonal modes [8]. This system exhibits an electromagnetic induced transparency.

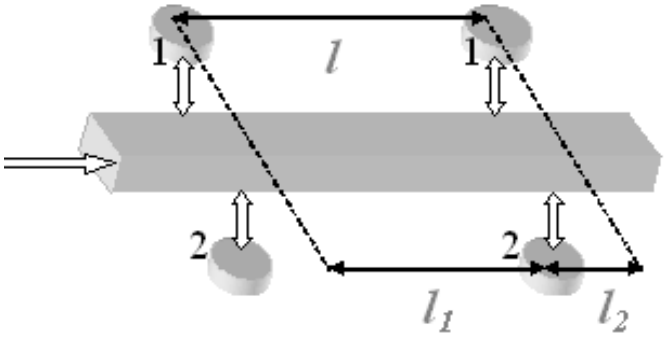

Fig.1. Schematic of two unit cells of the coupled-cavity structure used to stop light. The cavities couple to the waveguide with a coupling rate of $1/\tau_i$. Length of the unit cell is $l = l_1 + l_2$ [3].

2. TRIANGULAR GAAS LATTICES

The original system used to validate the theory is based on a square lattice with a dielectric constant of 12.25 [3]. The triangular lattice GaAs structure, suggested in a previous work [1], shows some advantages over the original one. These advantages are summarized below:

2.1 Effect of the triangular lattice

At the same background dielectric constant and center frequency, the triangular lattice shows an advantage of compressing larger bandwidths than that of the square one. In addition, the ratio of the final bandwidth (after modulation) to the original bandwidth (before modulation) is to the advantage of the triangular lattice. The reason for this behavior is two-fold [1]: first, because the photonic bandgap in the case of a triangular lattice is wider than that in the case of a square lattice, an introduced defect mode at the middle of each gap is more localized in the case of a triangular lattice. The evanescent modes in the gap of the structure have exponential nature and they share the same final value of leaking into the extended bands. Therefore, any deviation, represented by the refractive index modulation, is more effective in the case of the triangular lattice. This results in a wider pulse bandwidth to compress. The other factor arises from the fact that the mode is better localized in the photonic bandgap of the triangular lattice because it is wider than the square one. A better quality factor is, thus, obtained in the case of the triangular lattice. Both the preceding factors can be introduced in the bandwidth $\Delta \equiv 2Q|\omega_1-\omega_2|/\omega_0$ leading to a higher compressible bandwidth.

2.2 Effect of using GaAs

Using GaAs (ε=11.4 at λ=1.5μm [4]) leads to a larger compressible bandwidth than that obtained if the original material [1] with ε=12.25 is used. Because GaAs has a lower dielectric constant, it offers narrower photonic bandgap and is, thus, weak at the localization of cavity modes. This weakness can result into a higher bandwidth under the following circumstances. For a material with ε=12.25, a large value for dielectric shift $\Delta\varepsilon$ is required for a defect mode to cross half the bandgap (which is large) and be introduced at the middle of the gap. On the other hand, in the case of GaAs, no such big effort is required because the bandgap is smaller. If the difference in the original reference value is small ($\Delta\varepsilon$=12.25-11.14) and it will be further reduced when the refractive index modulation is considered (Δn=3.5-3.37), the required dielectric constant for the defect cavity mode can be larger for GaAs (n_{cavity}=2.42) than in the case of ε=12.25 (n_{cavity}=2.24) at the same defect frequency. Once the defect mode is established, the perturbation and variational theories can be applied. This is done in [1] and using GaAs shows a higher compressible bandwidth.

3. PARAMETERS OPTIMIZATION

The previously discussed model based on GaAs triangular lattices shows two main problems [1]; the first is the requirement of longer waveguide lengths for the compression of the extra band. In an attempt to solve this problem, there are two suggested scenarios [1]. The second problem is the higher group-velocity dispersion shown in the new design. The objective of this work is to address this problem.

In an attempt to solve this problem, the linear defect introduced in the forbidden bandgap is spanned searching for an appropriate range of linear group-velocity. At the same time, it should be as close as possible to the middle of the forbidden region for maximum localization of the defect mode. Zooming in Fig. 2 shows that a shift from the old center frequency ω_o=0.357 (Fig. 3 (a)) to the new one, ω_o=0.375 (Fig. 3 (b)) satisfies both conditions, especially when used with GaAs. The new range of operation shows a close approximation to the (almost) linear curve of the square lattice structure. All curves are calculated at the same refractive index modulation rate.

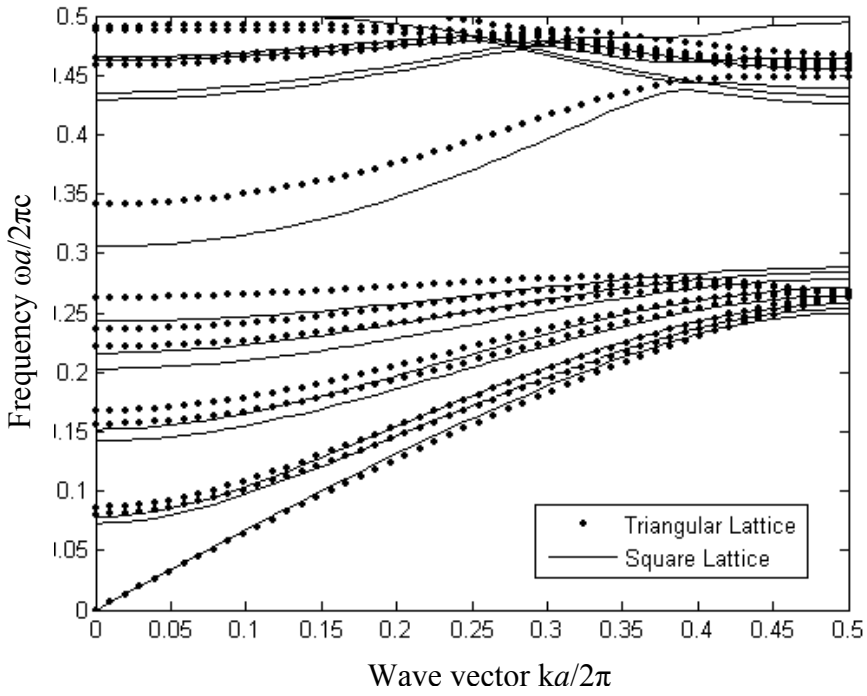

Fig. 2 The band structure of the linear defect (due to waveguide only) for a background dielectric constant of 11.4.

In order to produce no change in the center frequency of operation, the original model parameters should be redesigned; more specifically, the defect modes of the cavities. Moreover, by changing the center frequency, the condition for maximum transmission is violated and the transmission through the structure is reduced.

3.1 Defect optimization

In the previous designs, square lattice [3] and triangular lattice [1] structures, the center frequency is kept the same at a value of 0.357. This defect frequency is obtained by reducing both the radius to 0.1a for both structures and dielectric constant of a single rod to 5.8564 and 8.1796 for square and triangular lattices respectively. These calculations are done at a background dielectric of GaAs. In order to obtain a new center frequency of 0.375, only the dielectric constant is changed. The radius of the defect rod is kept untouched. This design, therefore, shows a fabrication advantage over the past two designs. In a GaAs background of triangular rods, reducing the dielectric constant of a single rod to 2.155 creates a single mode cavity of a resonance frequency ω_o=0.375.

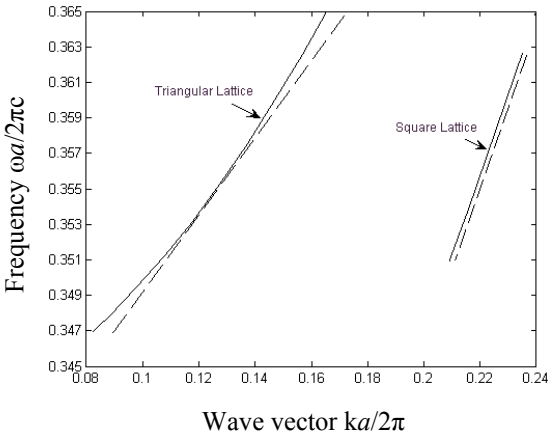

Fig. 3. (a) The original frequency range of operation (ω=0.357) is zoomed in and shown in relation to the perfect linear mode (dashed line)

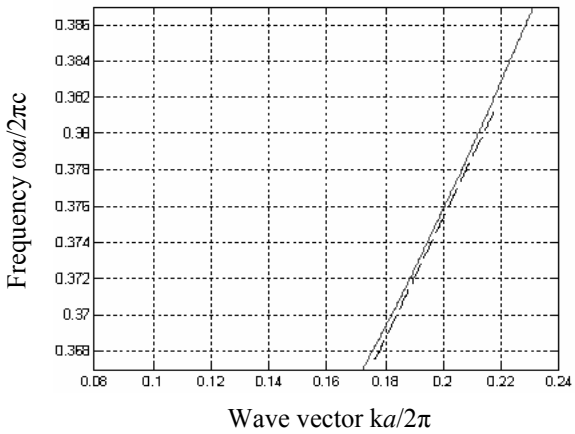

Fig. 3. (b) The new frequency region of operation (ω=0.375) is, again, zoomed in for a triangular lattice structure.

3.2 Cavities separation

The design of this coupled resonator array is dependent on the adjustment of the system components in such a way that the system shows an optical analogue to electromagnetically induced transparency. For maximum transmission through such a structure, the separation between the cavities should be adjusted such that the following equation is satisfied:

$$\mathbf{L}_1 = \frac{n\pi}{B(\omega)} \tag{1}$$

where B(ω) is the waveguide dispersion relation, and n is an integer. Equation (1) represents a condition for maximum transmission in the common problem of simple parallel mirrors resonator (like Fabry-Perot etalon).

An important characteristic of a photonic crystal based waveguide is that light is mainly directed in the low-ε regions which are usually air. As a result, the dispersion relation $\beta(\omega)$ can be approximated to (ω/c). This result and equation (1) at the operating frequency found above gives cavities separation of 4a for maximum transmission.

4. ANALYSIS OF THE OPTIMIZED MODEL

In order to give a comprehensive analysis of the discussed system, the transmission characteristics and band structure should be found. The intensity transmission coefficient, T, of this system is calculated as follows [5] [9] [10]

$$T = \left(\frac{|t_1 t_2|}{1 - |r_1 r_2|} \right)^2 \frac{1}{1 + 4\left(\sqrt{|r_1 r_2|} \Big/ \left(1 - |r_1 r_2|\right) \right)^2 \sin^2 \theta} \tag{2}$$

where 2θ is the round trip phase angle accumulated in the waveguide sections: $\theta = 0.5\mathrm{Arg}(r_1 r_2 e^{-2j\beta(\omega)l_1})$, $\beta(\omega)$ is the waveguide dispersion. r_i and t_i are the reflection and transmission coefficients of the i^{th} cavity given [5] by

$$r_i = \frac{\gamma}{j(\omega - \omega_i) + \gamma} \tag{3}$$

$$t_i = \frac{j(\omega - \omega_i)}{j(\omega - \omega_i) + \gamma} \tag{4}$$

In order to obtain the band structure of such a system, the transmission matrix should be found a priori. If T_{ci} and T_{li} are the transmission matrices for the i^{th} waveguide side coupled to a single resonator and waveguide section, respectively, (i=1, 2), the transmission matrix through an entire unit cell is found [11] to be

$$\mathrm{T} = \mathrm{T}_{c1}\mathrm{T}_{l1}\mathrm{T}_{c2}\mathrm{T}_{l2} \tag{5}$$

where

$$\mathrm{T}_{ci} = \begin{pmatrix} 1 + j/(\omega-\omega_i)\tau_i & j/(\omega-\omega_i)\tau_i \\ -j/(\omega-\omega_i)\tau_i & 1 - j/(\omega-\omega_i)\tau_i \end{pmatrix} \tag{6}$$

where ω_i, and $1/\tau_i$ are the resonance frequency and coupling rate to the waveguide for the i^{th} resonator and

$$\mathrm{T}_{li} = \begin{pmatrix} e^{-j\beta(\omega)l_i} & 0 \\ 0 & e^{j\beta(\omega)l_i} \end{pmatrix} \tag{7}$$

Using the above model, the band diagram for equal coupling rate cavities and ignoring any direct coupling between side cavities is found [11] to be

$$\frac{1}{2}Tr(\mathrm{T}) = \cos(kl) = f(\omega)$$
$$\equiv \cos(\beta l) + \frac{C+}{(\omega-\omega_1)} + \frac{C-}{(\omega-\omega_2)} \tag{8}$$

where

$$C\pm = \frac{\sin(\beta l)}{\tau} \pm \frac{2\sin(\beta l_1)\sin(\beta l_2)}{(\omega_1-\omega_2)\tau^2} \tag{9}$$

This analysis is based on the representation of the eigenvalues of T as $e^{-jk(\omega)l}$, and $e^{jk(\omega)l}$ (because det (T) =1); where k is the Bloch wavevector of the entire system.

5. SIMULATION RESULTS

The transmission characteristics for the system shown in Fig.1 with the new parameters are shown in Fig. 4 (a). The transmission characteristics are calculated using the parameters obtained from simulating these systems and using equations (2) – (4) at a center frequency of ω_o=0.375. Figure 4 (b) shows the band structure calculated using equations (5) – (9). This system exhibits three photonic bands. The width of the middle band depends strongly on the cavities resonant frequencies. By modulating the cavities frequency spacing, the system bandwidth is compressed. Figure 4 (b) shows the possibility of nearly flat band in the entire Brillouin zone of the structure. In this way, by cascading the bandwidth filters shown in Fig. 4 (a), it becomes possible to reduce the group velocity of the propagating pulse to zero. After the general behavior of the system is assessed, it is very important to compare these systems with the other systems previously discussed. Being an optimization process, the new system should combine the low group-velocity dispersion of the original square lattice at ε=12.25 and the higher compressible bandwidth of the triangular lattice structure of GaAs. The former has been taken into consideration in the system design. As shown in Fig. 5, the performance of the new design is comparable to that of the triangular lattice at ε=11.4 and r_{defect}=0.1a at ω_o=0.375.

6. CONCLUSION

This work represents an attempt to overcome the high group-velocity dispersion brought about by the introduction of triangular lattice in a previous work [1] to the dynamic light stoppage structure. Shifting the center frequency of operation from 0.357 to 0.375 represents a more linear region of operation. In this way, the problem of group-velocity dispersion is overcome and the performance of the system becomes close to that of the original model of a square lattice. As the center frequency is modified, the necessary condition for maximum transmission is violated and the transmission dropped below maximum. This problem is handled by redesigning the cavities separations so that the round trip phase angle accumulated in the resonator is an integral multiple of 2π. In this way, the transmission returned back to maximum

and the compressible bandwidth of the final structure is comparable to that of the triangular lattice at the original center frequency of 0.357.

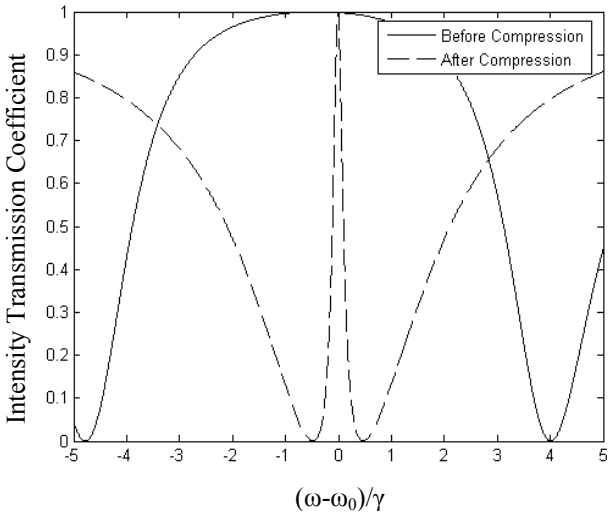

Fig. 4. (a) Transmission characteristics for a triangular lattice structures with ε=11.4 and ω_o=0.375

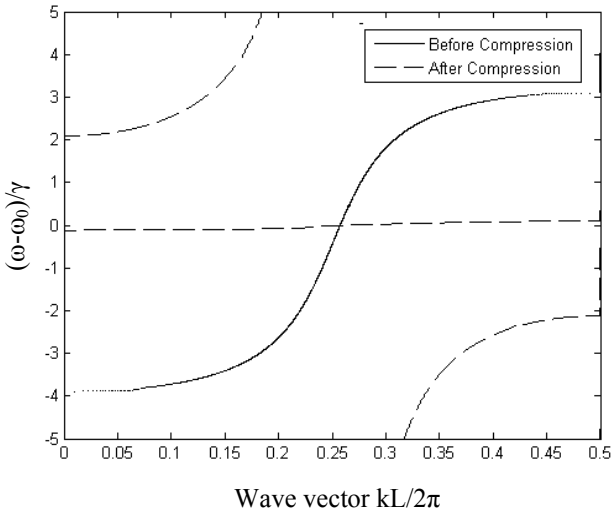

Fig. 4. (b) Band structure for a triangular lattice structures with ε=11.4 and ω_o=0.375

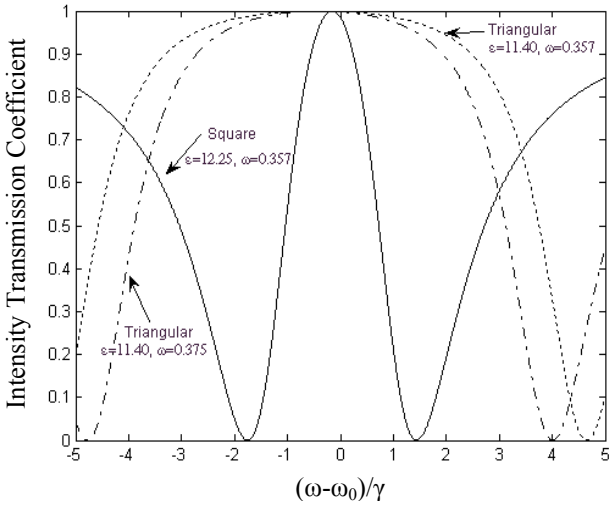

Fig. 5. (a) Transmission characteristics for a square lattice (ε=12.25, r_{defect}=0.1*a*), a triangular lattice (ε=11.4, r_{defect}=0.1*a*), and a triangular lattice (ε=11.4, r_{defect}=0.2*a*).

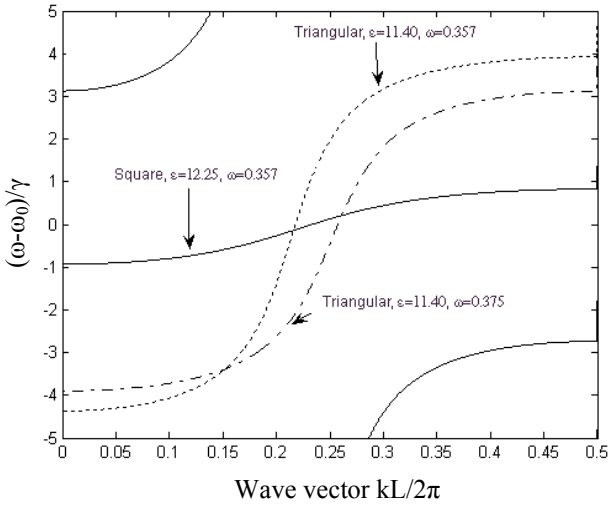

Fig. 5. (b) Band structure for a square lattice (ε=12.25, r_{defect}=0.1*a*), a triangular lattice (ε=11.4, r_{defect}=0.1*a*), and a triangular lattice (ε=11.4, r_{defect}=0.2*a*).

REFERENCES

[1] Shalaby, M., AboulSeoud, A. K., and Aly, M. H., "Dynamic Photonic Crystal Structures for Optical Storage and Processing Based on GaAs and Triangular Lattice," To be Published.

[2] Fan, S., Yanik, M. F., Povinelli, M. L., and Sandhu, S., "Dynamic Photonic Crystals," Optics and Photonics News, 18, 41-45 (2007).

[3] Fan, S. and Yanik, M. F., "Dynamic Photonic Structures: Stopping, Storage, and Time-Reversal of Light," Studies in Applied Mathematics, 115, 233-254 (2005).
[4] Joannopoulos, J.D., Johnson, S.G., Winn, J.N., and Meade, R.D., [Photonic Crystals: Molding the Flow of Light], 2nd ed., Princeton University Press, USA (2008).
[5] Fan, S., "Manipulating Light with Photonic Crystals," Physica B 394, 221–228 (2007).
[6] Yanik, M. F., Suh, W., Wang, Z., and Fan, S., "Stopping Light in a Waveguide with an All-Optical Analogue of Electromagnetic Induced Transparency," Phy. Rev. Lett., 93, 233903 (2004).
[7] Yanik, M. F. and Fan, S., "Stopping and Storing Light Coherently," Phy. Rev. A, 71, 013803 (2005).
[8] Suh, W., Wang, Z., and Fan, S., "Temporal Coupled-Mode theory and the Presence of Non-Orthogonal Modes in Lossless Multi-Mode Cavities," IEEE J. Quantum Electron., 40, 1511-1518 (2004).
[9] Xu, Q., Sandhu, S., Povinelli, M.L., Shakya, J., Fan, S., and Lipson, M., "Experimental Realization of an On-chip All-Optical Analogue to Electromagnetically Induced Transparency," Phy. Rev. Lett., 96, 123901 (2006).
[10] Fan, S., Suh, W., Joannopoulos, J.D., and Suh, W., "Temporal Coupled-Mode Theory for the Fano Resonance in Optical Resonators," J. Opt. Soc. Am. A, 20, 569-572 (2003).
[11] Fan, S., Yanik, M. F., Wang, Z., Sandhu, S., and Povinelli, M.L., "Advances in the Theory of Photonic Crystals," IEEE J. Lightwave Technol., 24, 4493-4501 (2006).